

Resolution of Microscopic Protonation Enthalpies of Polyprotic Molecules by Means of Cluster Expansions

Michal Borkovec*

Department of Inorganic, Analytical, and Applied Chemistry, University of Geneva, 30 Quai Ernest-Ansermet, 1205 Geneva, Switzerland

Duško Čakara

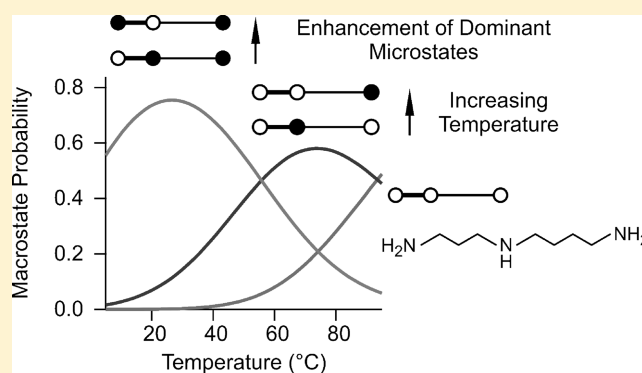
Department of Biotechnology, University of Rijeka, Brice Mazuranica 10, 51000 Rijeka, Croatia

Ger J. M. Koper

Department of Chemical Engineering, Delft University of Technology, PO Box 5045, 2600 GA Delft, The Netherlands

S Supporting Information

ABSTRACT: Cluster expansion techniques are used to obtain microconstants and microenthalpies of protonation reactions. The approach relies on the analysis of macroscopic protonation constants and protonation enthalpies within a homologous series. Various linear aliphatic polyamines are considered, including 3,4-tri (spermidine), 3,4,3-tet (spermine), and 2,2,2,2-pent. Besides the full resolution of the microscopic protonation equilibria, one obtains information on the temperature dependence of the microstate probabilities. We find that the concentrations of the dominant microspecies increase with increasing temperature. Due to the large negative protonation enthalpies that are typical for amines, higher temperatures generally favor the less protonated species.



1. INTRODUCTION

Polyprotic acid–base reaction equilibria are normally discussed from the *macroscopic* point of view. This picture provides information concerning the number of protons bound, the so-called *macrostates*, and their relative populations through the respective macroscopic equilibrium constants, the *macroconstants*. While such a macroscopic approach is simple to handle, it does not provide any chemically relevant information concerning the protonation state of the individual ionizable groups within the molecule. In order to obtain such information, one must discuss the equilibria from the *microscopic* point of view. This picture provides information on which groups are being protonated and which are not, the so-called *microstates*. One can obtain their relative populations through the respective microscopic equilibrium constants, the *microconstants*. The microscopic picture is essential to understand a wide variety of chemical phenomena, including self-assembly,^{1–3} ligand–receptor interactions,^{4,5} folding kinetics,⁶ or chemical reaction networks.⁷ The microscopic point of view is equally essential to rationalize ionization constants estimated from *ab initio* computational schemes.^{8,9} However, many chemists remain uneasy with the microscopic approach as

they suspect that for more complex molecules the determination of the microconstants represents a daunting task.

The situation has changed substantially with the development of cluster expansion techniques for the description of microscopic equilibria.^{10–19} These techniques permit one to parametrize the large number of microconstants in terms of a much smaller number of cluster parameters. These parameters include one microconstant per ionizable group and a set of interaction parameters, which characterize the influence of neighboring groups. These parameters may further satisfy simple group additivity relationships, and their number can be substantially reduced by exploiting molecular symmetries. Such cluster expansion techniques permit one to determine relative populations of the various microstates including all microconstants, even for larger molecules, including linear amines,^{10,11,13} complexing agents,^{18–20} polyphosphates,^{14,15} and dendrimers.^{12,16,17} Such microequilibria can be resolved from macroscopic titration data of single molecules of high symmetry only. Successful general strategies can rely on site-

Received: February 6, 2012

Revised: February 26, 2012

Published: March 1, 2012

specific titration curves determined by nuclear magnetic resonance (NMR)^{11–15,18–23} or on macroscopic titration data of a homologous series.^{10,16,17} An essential lesson taught by the cluster expansion techniques is that a useful parametrization of the problem is not given in terms of the large number of microconstants, but rather by the much smaller set of cluster parameters, which include one microconstant per site and normally a small number of interaction parameters. Another advantage of the cluster techniques is that they can be readily extended to macromolecules (i.e., proteins, polyelectrolytes, dendrimers).^{16,17,24–29} These techniques can be adapted to a larger number of ionizable sites in a straightforward fashion, while such situations cannot be easily handled within the classical macroscopic picture.

This cluster expansion approach was recently extended to investigate how other degrees of freedom influence the binding of protons on a microscopic level. From the coupling between ionization and conformations, one can obtain a systematic description of the rotational microstates, the so-called *rotomicrostates*.^{20,30} Another extension pursued competitive binding phenomena, for example, involving metal ions and protons³¹ as well as different types of metal ions.^{31–34}

Temperature effects on microscopic ionization equilibria have rarely been investigated. To our knowledge, only limited information on diprotic hydroxypyridines is available so far.^{35–37} The generalization of the cluster approach to include temperature effects should enable us to perform this type of analysis in more complex situations. The present approach explores a similar interpretation of enthalpy effects in surfactant binding.³⁸ An analogous framework can be put forward based on the cluster expansion to include temperature and enthalpy effects. For the first time, this development allows us to obtain all microscopic enthalpies of ionization reactions in polyprotic molecules and to estimate the temperature dependence of the relative microstate populations.

2. PROTONATION OF POLYPROTIC MOLECULES

A general statistical mechanical framework to describe the microscopic protonation equilibria of polyprotic molecules is based on cluster expansions presented earlier.^{10,11,39} Since this development is essential for the following, a brief summary is given here.

Consider a polyprotic molecule with N ionizable sites. The protonation state of a site i can be defined by introducing an occupation variable s_i , whereby $s_i = 1$ when the site is protonated and $s_i = 0$ when deprotonated ($i = 1, 2, \dots, N$). The microscopic protonation state (or microstate) of the entire molecule is specified by the set of these variables s_1, s_2, \dots, s_N abbreviated as $\{s_i\}$. To each microstate one can assign a free energy $F(\{s_i\})$ that will be expressed per unit mole whereby the fully deprotonated state is chosen as the reference state. In a dilute solution, the polyprotic molecule can be described by the semigrand partition function

$$\Xi = \sum_{\{s_i\}} a_{\text{H}}^n e^{-\beta F(\{s_i\})} \quad (1)$$

where a_{H} is the proton activity, $\beta = 1/RT$ with T being the absolute temperature and R being the gas constant to set the energy scale relative to one mole, and

$$n = \sum_{i=1}^N s_i \quad (2)$$

is the total number of protons bound. In the solution chemistry literature, one normally abbreviates $\text{pH} = -\log_{10} a_{\text{H}}$. All quantities of interest can be obtained from the corresponding thermal average

$$\langle \dots \rangle = \Xi^{-1} \sum_{\{s_i\}} a_{\text{H}}^n e^{-\beta F(\{s_i\})} \dots \quad (3)$$

Provided the free energies for all microstates are known, all quantities can be evaluated by direct enumeration.^{10–12}

Polyprotic molecules are commonly described in terms of macroscopic protonation states, or macrostates. A macrostate defines the total number of protons bound, but does not provide any information whether a given site is protonated or not. The above microscopic treatment can be best related to the macroscopic picture by realizing that the partition function can be written as a fugacity expansion

$$\Xi = \sum_{n=0}^N \bar{K}_n a_{\text{H}}^n \quad (4)$$

where the expansion coefficients are the cumulative macroconstants

$$\bar{K}_n = \sum_{\{s_i\}} \delta_n \sum_i s_i e^{-\beta F(\{s_i\})} \quad (5)$$

where δ_{ij} is the Kronecker delta, and $\bar{K}_0 = 1$. In the biochemistry literature, the fugacity expansion is known as the binding polynomial.^{18,40} The commonly used stepwise macroconstants are given by $\text{p}K_n = \log(\bar{K}_n/\bar{K}_{n-1})$. The average number of bound protons ν is accessible from a potentiometric titration experiment and can be expressed by the thermodynamic derivative

$$\nu = \left(\frac{\partial \ln \Xi}{\partial \ln a_{\text{H}}} \right)_{\beta} \quad (6)$$

or as the statistical average

$$\nu = \langle n \rangle = \sum_{n=0}^N n P_n(a_{\text{H}}) \quad (7)$$

Thereby, we have introduced the macrostate probability

$$P_n(a_{\text{H}}) = \Xi^{-1} \bar{K}_n a_{\text{H}}^n = \frac{\bar{K}_n a_{\text{H}}^n}{\sum_{n=0}^N \bar{K}_n a_{\text{H}}^n} \quad (8)$$

Since the number of microstates grows as 2^N with the number of ionizable sites, the number of free energies $F(\{s_i\})$ needed to describe all microstates can become very large. Therefore, these free energies do not represent a useful parametrization of the problem. It is much more practical to consider the so-called cluster expansion commonly used in the

statistical mechanics literature.⁴¹ One makes a series expansion of the free energy in terms of the discrete state variables s_i as

$$\frac{\beta F(\{s_i\})}{\ln 10} = -\sum_i p\hat{K}_i s_i + \frac{1}{2!} \sum_{i,j} \varepsilon_{ij} s_i s_j + \frac{1}{3!} \sum_{i,j,k} \lambda_{ijk} s_i s_j s_k + \dots \quad (9)$$

where $p\hat{K}_i$ is the logarithm of the microscopic protonation constant when all other sites are deprotonated, ε_{ij} is the pair interaction parameter, and λ_{ijk} is the triplet interaction parameter. The factor of $\ln 10$ has been introduced to ensure that the parameters introduced are simply related to the pH scale. The interaction parameters ε_{ij} and λ_{ijk} are symmetric upon exchange of any of the two indices, and they vanish whenever two indices are equal. This cluster expansion splits the free energy into additive contributions of small clusters of sites, namely of single sites, their pairs, triplets and so on. While in the general case this involves $2^N - 1$ cluster parameters, one expects that higher order contributions as well as contributions involving distant sites should be negligible. For this reason, the set of cluster parameters necessary to describe all microspecies will only involve the microscopic protonation constants $p\hat{K}_i$ as well as some of the interaction parameters for pairs ε_{ij} and eventually few triplets λ_{ijk} . Their number can be further reduced by exploiting molecular symmetries. In our opinion, these cluster parameters represent the most suitable parametrization of microscopic protonation equilibria available today.

A given macrostate n is composed of those microstates that have the same number of protons bound. The probability (or mole fraction) of a microstate within a given macrostate is independent of pH and can be expressed by a conditional microstate probability

$$\pi_n(\{s_i\}) = \bar{K}_n^{-1} e^{-\beta F(\{s_i\})} \quad (10)$$

When the list of microstates is ordered according to decreasing probability, the top entries in this list reflect the dominant microstates. The commonly used microscopic equilibrium constants can be equally used to define all microstates unambiguously. These constants refer to the reaction where the deprotonated site i is being protonated but all other sites retain the same protonation state. The corresponding protonation equilibrium can be written as



where $\{s_k\} = s_1, \dots, s_{i-1}, 0, s_{i+1}, \dots, s_N$ and $\{s'_k\} = s_1, \dots, s_{i-1}, 1, s_{i+1}, \dots, s_N$. The respective microscopic constant can be expressed as

$$p\hat{K}_{A\{s_k\}} = \frac{\beta F(\{s'_k\}) - \beta F(\{s_k\})}{\ln 10} \quad (12)$$

Inserting eq 9 into eq 12 and observing that one can write $s'_k = s_k + \delta_{ik}$, one obtains

$$p\hat{K}_{A\{s_k\}} = p\hat{K}_i - \sum_j \varepsilon_{ij} s_j - \frac{1}{2} \sum_{j,k} \lambda_{ijk} s_j s_k + \dots \quad (13)$$

Therefore, all $N2^{N-1}$ microscopic ionization constants can be evaluated once the cluster parameters are known. The number of cluster parameters is always smaller than the number of microconstants, especially when further simplifications are being made. The parametrization in terms of the cluster

parameters is not only simpler but also more intuitive. While microscopic equilibria can be defined in terms of all possible microconstants, this set contains redundant information and is cumbersome to use. The natural parametrization is given in terms of the cluster parameters, all of which are independent. When eq 13 is truncated after the pair interaction term, it is analogous to the Taft relation used in organic chemistry.⁴² However, the latter approach is useful for molecules with small number of ionizable sites, and becomes difficult to use for larger molecules. More details on these cluster expansion techniques are given elsewhere.^{10,11,39}

3. MICROSCOPIC REACTION ENTHALPIES

The present framework can be extended to the treatment of heat effects in a straightforward fashion. The reaction enthalpy can be obtained from the temperature derivative of the partition function³⁸

$$h = - \left(\frac{\partial \ln \Xi}{\partial \beta} \right)_{a_H} \quad (14)$$

where $\beta = 1/RT$. Since the second cross-derivatives of any partition function are equal, the following Maxwell relation⁴³ must hold:

$$- \left(\frac{\partial h}{\partial \ln a_H} \right)_\beta = \left(\frac{\partial \nu}{\partial \beta} \right)_{a_H} \quad (15)$$

This relation states that the dependence of the reaction enthalpy on the proton activity is the same as the temperature dependence of the adsorption isotherm. In other words, one obtains the same information from a calorimetric experiment and a temperature-dependent potentiometric titration experiment.

By inserting eqs 1 and 3 into eq 14 and evaluating the derivative, one recognizes that the enthalpy of a microstate is given by

$$\xi(\{s_i\}) = \frac{\partial [\beta F(\{s_i\})]}{\partial \beta} \quad (16)$$

The overall reaction enthalpy given in eq 14 can be thus represented as the statistical average

$$h = \langle \xi \rangle = \sum_n \bar{H}_n p_n(a_H) \quad (17)$$

whereby the entering coefficients are the cumulative macroscopic enthalpies of reaction that are given by

$$\bar{H}_n = - \frac{\partial \ln \bar{K}_n}{\partial \beta} = \bar{K}_n^{-1} \sum_{\{s_i\}} \delta_n \sum_i s_i e^{-\beta F(\{s_i\})} \xi(\{s_i\}) \quad (18)$$

and $\bar{H}_0 = 0$. They are commonly expressed as the stepwise reaction enthalpies $H_n = \bar{H}_n - \bar{H}_{n-1}$.

The microscopic reaction enthalpy in eq 16 can be equally expressed in terms of a cluster expansion. By taking the corresponding temperature derivative of eq 9, one obtains

$$\xi(\{s_i\}) = \sum_i \hat{H}_i s_i - \frac{1}{2!} \sum_{i,j} g_{ij} s_i s_j - \frac{1}{3!} \sum_{i,j,k} l_{ijk} s_i s_j s_k + \dots \quad (19)$$

whereby we have introduced the microscopic enthalpies, or briefly, microenthalpies,

$$\hat{H}_i = - \frac{\partial \ln \hat{K}_i}{\partial \beta} = - \ln 10 \frac{\partial p\hat{K}_i}{\partial \beta} \quad (20)$$

the pair contributions to the enthalpy, or pair enthalpies,

$$g_{ij} = - \ln 10 \frac{\partial \varepsilon_{ij}}{\partial \beta} \quad (21)$$

and finally triplet contributions to the enthalpy, or triplet enthalpies,

$$l_{ijk} = - \ln 10 \frac{\partial \lambda_{ijk}}{\partial \beta} \quad (22)$$

The same symmetry relations introduced for the interaction parameters also apply to the interaction enthalpies. The entire set of these parameters, namely microenthalpies, pair, and triplet enthalpies, will be referred to as the *cluster enthalpies*.

The temperature dependence of the cluster parameters can be therefore approximated as

$$\begin{aligned} p\hat{K}_i &= p\hat{K}_i^{(0)} - \frac{\hat{H}_i}{\ln 10} (\beta - \beta^{(0)}) \\ \varepsilon_{ij} &= \varepsilon_{ij}^{(0)} - \frac{g_{ij}}{\ln 10} (\beta - \beta^{(0)}) \\ \lambda_{ijk} &= \lambda_{ijk}^{(0)} - \frac{l_{ijk}}{\ln 10} (\beta - \beta^{(0)}) \end{aligned} \quad (23)$$

where the quantities with superscript (0) refer to the standard temperature of 25 °C. The temperature dependence of all relevant probabilities can be evaluated too. In particular, the temperature dependence of the conditional microstate probabilities is given by

$$\frac{\partial \pi_n}{\partial \beta} = (\xi - \bar{H}_n) \pi_n \quad (24)$$

In analogy to the microconstant, one can introduce the microenthalpies as

$$\hat{H}_{A\{s_k\}} = \xi(\{s'_k\}) - \xi(\{s_k\}) \quad (25)$$

Inserting eq 19 into eq 25 and observing that $s'_k = s_k + \delta_{ik}$, one obtains

$$\hat{H}_{A\{s_k\}} = \hat{H}_i - \sum_j g_{ij} s_j - \frac{1}{2} \sum_{j,k} l_{ijk} s_j s_k + \dots \quad (26)$$

Therefore, once the cluster enthalpies are known, all possible microenthalpies can be evaluated. Again, the set of all microscopic enthalpies represents a cumbersome and redundant parametrization of these equilibria, and the natural parametrization is given in terms of the cluster enthalpies. Expressions simplify substantially for identical and non-interacting sites,³⁸ but this situation is relatively rare. More information on this topic is given in the Supporting Information.

5. ILLUSTRATIVE EXAMPLES

This section will illustrate the full resolution of microenthalpies for some polyprotic molecules and their chemical significance. We always rely on macroscopic constants pK_n and macroscopic

enthalpies H_n tabulated in a database.⁴⁴ Such macroscopic data are obtained from potentiometric titrations and calorimetric experiments. Microenthalpies can be also deduced from data on single highly symmetric molecules, in particular, symmetric diprotic acids and bases. Examples of this kind are presented in the Supporting Information. NMR titration curves obtained at different temperatures should be equally suitable to obtain information on microenthalpies, but this approach will not be explored here.

Figure 1 shows the two homologous series of linear aliphatic amines investigated here. We will first focus on the family with

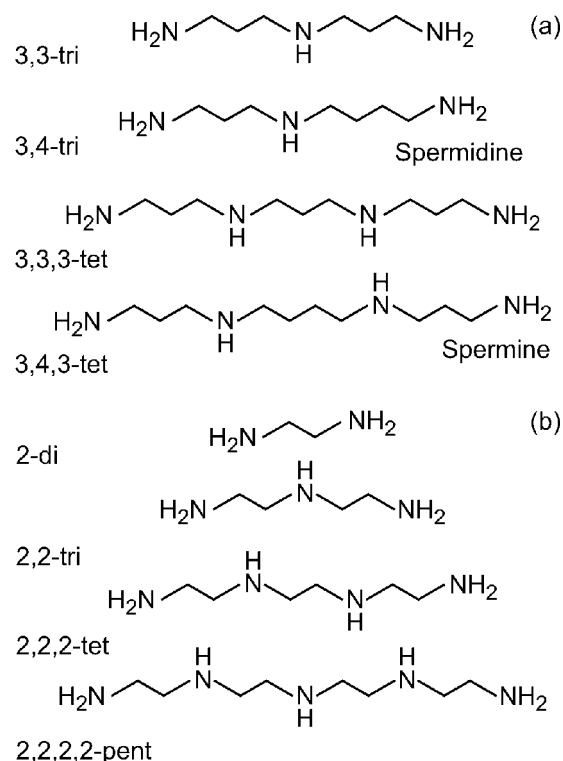


Figure 1. Two homologous series of aliphatic polyamines discussed in this study. (a) Propyl and butyl bridges, and (b) ethyl bridges.

propyl and butyl bridges, which includes the biologically relevant linear amines 3,4-tri (spermidine) and 3,4,3-tet (spermine).^{45,46} In this case, the cluster expansion converges rapidly due to the relatively larger distance between the ionizable groups. The second example will involve the series with ethyl bridges 2-di, 2,2-tri, 2,2,2-tet, and 2,2,2,2-pent. In this case, the distance between the ionizable groups is smaller, and therefore higher order interactions must be invoked. The solution properties of such aliphatic amines have been reviewed elsewhere.⁴⁶

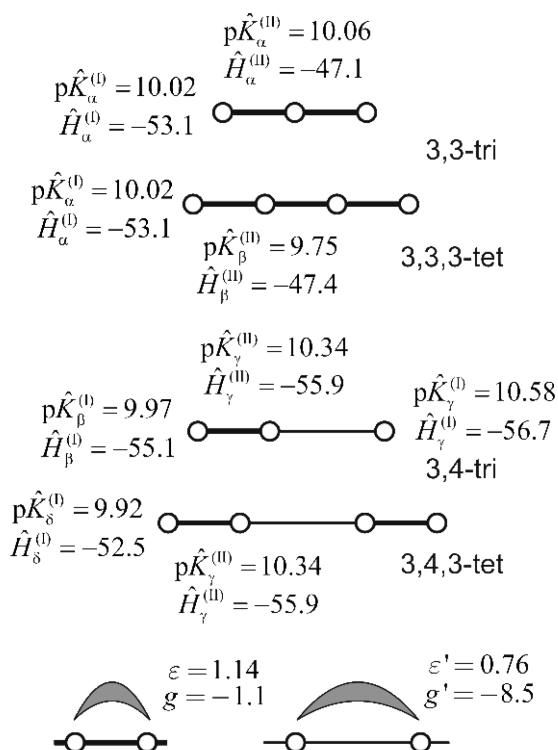
First, let us focus on 3,4-tri (spermidine) and 3,4,3-tet (spermine). The microscopic protonation constants of 3,4,3-tet were recently resolved with the cluster expansion technique from ¹³C NMR titration data by Frassinetti et al.¹³ Here we will demonstrate that comparable information on microconstants as well as on the microenthalpies can be obtained by analyzing a homologous series of macroscopic constants and enthalpies. The series at our disposal is 3,3-tri, 3,4-tri, 3,3,3-tet, and 3,4,3-tet (Table 1). The macroscopic constants and enthalpies are calculated in terms of the cluster parameters from eqs 5 and 18, and these parameters are determined by a least-squares fit. The

Table 1. Experimental and Fitted Macroscopic Protonation Constants and Enthalpies for Linear Amines with Propyl and Butyl Bridges at an Ionic Strength of 0.1 M^a

| molecule | <i>n</i> | macroconstants pK_n | | | macroenthalpies H_n (kJ/mol) | | |
|---|----------|-----------------------|-------|-------|--------------------------------|-------|-------|
| | | exp. ^b | calc. | diff. | exp. ^b | calc. | diff. |
| 1,5,9-triazanonane 3,3-tri | 1 | 10.65 | 10.51 | +0.14 | −51.4 | −51.0 | −0.4 |
| | 2 | 9.57 | 9.59 | −0.02 | −53.9 | −54.3 | +0.4 |
| | 3 | 7.68 | 7.72 | −0.04 | −45.6 | −45.9 | +0.3 |
| 1,5,10-triazadecane 3,4-tri, spermidine | 1 | 10.85 | 10.84 | +0.01 | −56.4 | −56.2 | −0.2 |
| | 2 | 9.85 | 9.87 | −0.02 | −53.5 | −53.4 | −0.2 |
| | 3 | 8.37 | 8.28 | +0.09 | −48.9 | −48.5 | −0.4 |
| 1,5,9,13-tetraazatridecane 3,3,3-tet, thermine | 1 | 10.48 | 10.51 | −0.03 | −51.0 | −51.1 | +0.1 |
| | 2 | 9.84 | 9.87 | −0.03 | −52.3 | −51.9 | −0.4 |
| | 3 | 8.51 | 8.59 | −0.08 | −48.9 | −49.2 | +0.3 |
| | 4 | 7.22 | 7.15 | +0.07 | −45.6 | −45.5 | −0.2 |
| 1,5,10,14-tetraazatetradecane 3,4,3-tet, spermine | 1 | 10.78 | 10.80 | −0.02 | −54.8 | −54.9 | +0.1 |
| | 2 | 9.98 | 9.99 | −0.01 | −51.8 | −52.3 | +0.5 |
| | 3 | 8.85 | 8.81 | +0.04 | −51.8 | −51.2 | −0.6 |
| | 4 | 7.90 | 7.99 | −0.09 | −47.6 | −47.8 | +0.2 |

^aTheir structures are given in Figure 1a. ^bExperimental data taken from a database.⁴⁴

parametrization of the problem together with the best fit results is presented in Table 1 and Figure 2. Our model assumes

**Figure 2.** Best fit cluster constants and cluster enthalpies for 3,3-tri, 3,4-tri, 3,3,3-tet, and 3,4,3-tet at an ionic strength of 0.1 M. The cluster enthalpies are reported in kJ/mol.

nearest-neighbor pair interactions only, which is in analogy with the model presented by Frassinetti et al.¹³ The fitted macroconstants and macroenthalpies are given in Table 1. One observes that the model describes the data very well, probably within experimental error.

Within the homologous series, one can distinguish five different primary amine groups based on their chemical environments. However, we assume that the microconstants and the microenthalpies of the primary amines for 3,3-tri and

3,3,3-tet are the same, which leaves us with four microconstants and four microenthalpies for primary amines, namely, $pK_\alpha^{(I)} = 10.02$ and $H_\alpha^{(I)} = -53.1$ kJ/mol (in 3,3-tri and 3,3,3-tet), $pK_\beta^{(I)} = 9.97$ and $H_\beta^{(I)} = -55.1$ kJ/mol (in 3,4-tri), $pK_\gamma^{(I)} = 10.58$ and $H_\gamma^{(I)} = -56.7$ kJ/mol (in 3,4-tri), and $pK_\delta^{(I)} = 9.92$ and $H_\delta^{(I)} = -52.5$ kJ/mol (in 3,4,3-tet). There are additionally four different secondary amines, but we assume that microconstants and the microenthalpies of the secondary amines in 3,4-tri and 3,4,3-tet are the same. That leaves us with three microconstants and three microenthalpies for the secondary amines, namely, $pK_\alpha^{(II)} = 10.06$ and $H_\alpha^{(II)} = -47.1$ kJ/mol (in 3,3-tri), $pK_\beta^{(II)} = 9.75$ and $H_\beta^{(II)} = -47.4$ kJ/mol (in 3,3,3-tet), and $pK_\gamma^{(II)} = 10.34$ and $H_\gamma^{(II)} = -55.9$ kJ/mol (in 3,4-tri and 3,4,3-tet). Due to the large distances between the amine groups, only nearest-neighbor interactions are taken into account. This leads to the pair interaction $\epsilon = 1.14$ and pair enthalpy $g = -1.1$ kJ/mol across a propyl $N-(CH_2)_3-N$ bond and $\epsilon' = 0.76$ and $g' = -8.5$ kJ/mol across a butyl $N-(CH_2)_4-N$ bond. These values should be compared with results from NMR titrations obtained for 3,4,3-tri, where the values $pK_\delta^{(I)} = 10.45$, $pK_\gamma^{(II)} = 10.48$, $\epsilon = 1.40$ were found,¹³ while based on the analysis of the homologous series 3-di, 3,3-tri, and 3,3,3-tet $pK_\alpha^{(I)} = 10.07$, $pK_\alpha^{(II)} \approx pK_\beta^{(II)} = 9.70$, $\epsilon = 1.05$ were reported.¹⁰ In spite of the differences in the medium, these values compare quite well to the values obtained from the present analysis. Especially the agreement with the fully independent NMR data suggests that the present analysis is reliable indeed. On the basis of these results, let us discuss the microscopic protonation mechanism and its temperature dependence for the biologically relevant 3,4-tri (spermidine) and 3,4,3-tet (spermine).

The protonation mechanism of 3,4-tri (spermidine) is summarized in Figure 3. The classical speciation diagram presents the relative concentration of each macrospecies as a function of pH (Figure 3a). One observes that the species with intermediate number of protons bound dominate the pH region 8–10. Thereby, the species with two protons bound is slightly more prevalent than the one with one proton bound. A similar diagram can also be presented as function of the temperature, but since the constants do not vary much with temperature, more modest variations of the macrostate probabilities are observed (Figure 3b). Dominant macrospecies

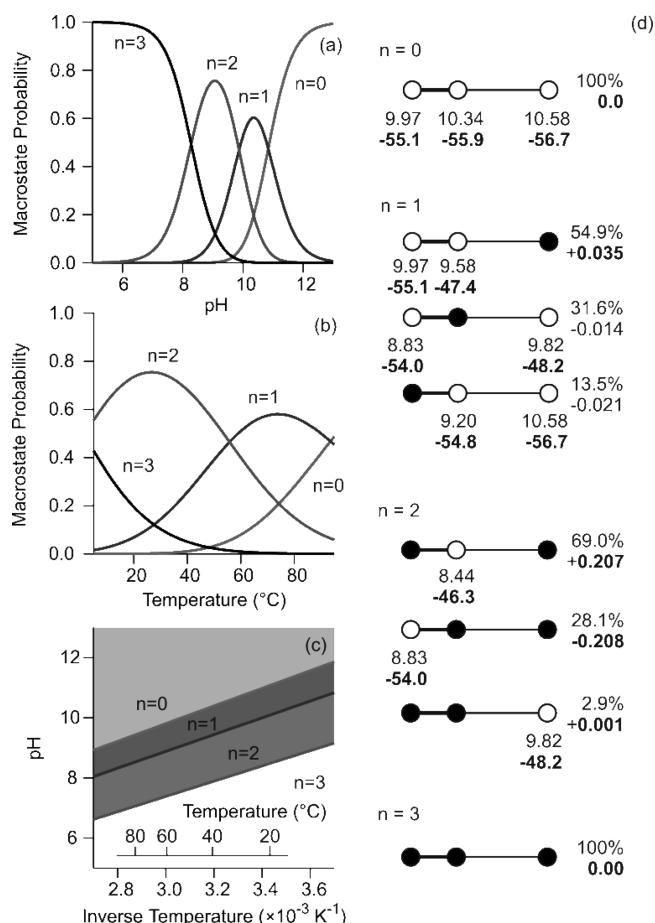


Figure 3. Protonation mechanism of 3,4-tri (spermidine) at an ionic strength of 0.1 M. Macrostate probabilities for various number n of protons bound (a) as a function of pH at 25 °C and (b) as a function of temperature at pH 9.0. (c) Dominant macrospecies as revealed in the van 't Hoff prevalence diagram. (d) Microstates ordered according to the number n of protons bound, whereby (●) refers to a protonated site, while (○) refers to a deprotonated one. The conditional microstate probability (in %) and its temperature coefficient (bold, in %K⁻¹) are shown on the right. Below each deprotonated site the respective microconstant and microenthalpy (bold, in kJ/mol) are given.

can also be represented in a van 't Hoff prevalence diagram since the condition of equal macrostate probabilities

$$P_n(a_H) = P_{n-1}(a_H) \quad (27)$$

leads to the simple relation that

$$\text{pH} = \text{p}K_n \quad (28)$$

Thus, plotting the macroscopic constants as a function of the inverse absolute temperature, one obtains straight lines that separate the regions of dominant macrospecies (Figure 3c). One observes that a temperature increase leads to deprotonation. This fact is related to the large negative reaction enthalpy of the amine group.

The microscopic protonation mechanism and its temperature dependence for 3,4-tri is summarized in Figure 3d. The dominant singly protonated species is the one where the propyl-amine group is protonated, but the other two species also occur at substantial concentrations. Their relative distribution is rather insensitive to temperature, as indicated by the small temperature dependence of the microstate

probabilities. The prevalent microspecies with two bound protons is the one where both primary amine groups are protonated, and the one with protonated amines around the propyl chain is also important. A temperature increase leads to a substantial enhancement of the most prevalent species. From the coefficient $\partial\pi/\partial T = 2.07 \times 10^{-3} \text{ K}^{-1} = 0.207\% \text{ K}^{-1}$ given in Figure 3d ($n = 2$) one finds that, upon a temperature increase from 25° to 65 °C, the microstate probability increases from 69% to 77%. For each deprotonated group of each microspecies, the corresponding microconstant and microenthalpy is also indicated. While such numbers are commonly considered to be necessary for the characterization of the microscopic equilibria, the corresponding cluster parameters contain the same information, and their meaning is more intuitive.

The protonation mechanism of 3,4,3-tet (spermine) is illustrated in Figure 4. The three intermediate macrostates all occur at similar concentrations in the pH range 8–10 (Figure 4a). By increasing the temperature, the distribution of these macrostates shifts toward the less protonated ones (Figure 4b). The situation can be also summarized in the van 't Hoff prevalence diagram (Figure 4c). The microspecies are shown in

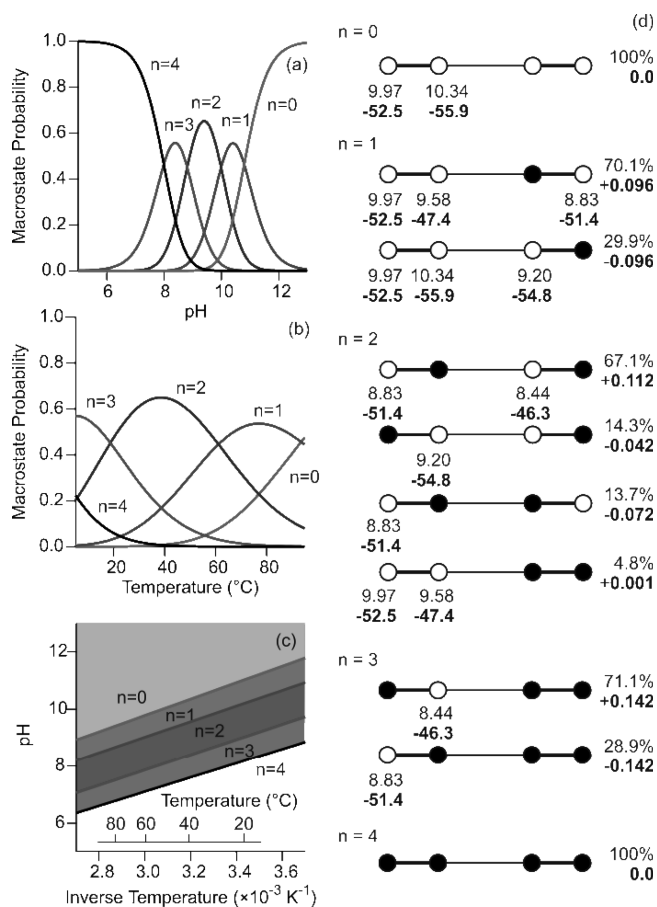


Figure 4. Protonation mechanism of 3,4,3-tet (spermine) at an ionic strength of 0.1 M. Macrostate probabilities for various number n of protons bound (a) as a function of pH at 25 °C and (b) as a function of temperature at pH 9.0. (c) Dominant macrospecies as revealed in the van 't Hoff prevalence diagram. (d) All microstates ordered according to the number n of protons bound. The conditional microstate probability (in %) and its temperature coefficient (bold, in %K⁻¹) are shown on the right. Below each deprotonated site, the respective microconstant and microenthalpy (bold, in kJ/mol) are given.

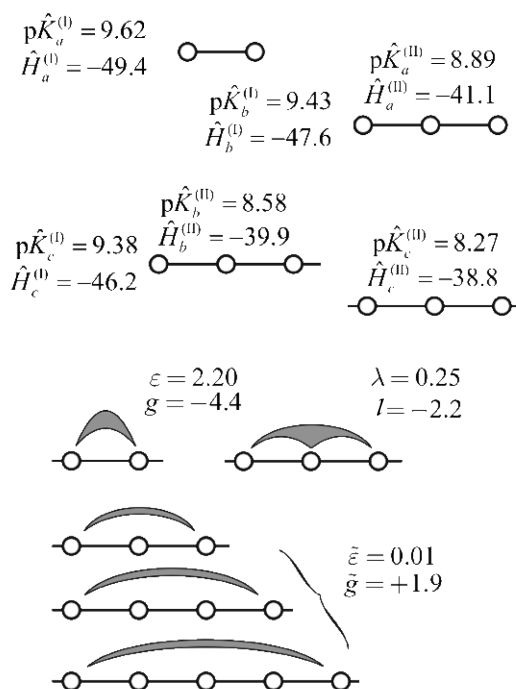
Table 2. Experimental and Fitted Macroscopic Protonation Constants and Enthalpies for Linear Amines with Ethyl Bridges at an Ionic Strength of 0.1 M^a

| molecule | <i>n</i> | macroconstants pK_n | | | macroenthalpies H_n (kJ/mol) | | |
|--|----------|-----------------------|-------|-------|--------------------------------|-------|-------|
| | | exp. ^b | calc. | diff. | exp. ^b | calc. | diff. |
| ethylenediamine 2-di | 1 | 9.92 | 9.92 | 0.00 | −49.3 | −49.4 | +0.1 |
| | 2 | 7.11 | 7.12 | −0.01 | −45.1 | −45.0 | −0.1 |
| 1,4,7-triazaheptane 2,2-tri | 1 | 9.84 | 9.79 | +0.05 | −46.8 | −46.8 | 0.0 |
| | 2 | 9.02 | 9.06 | −0.04 | −50.2 | −50.3 | +0.1 |
| | 3 | 4.25 | 4.24 | +0.01 | −30.0 | −30.2 | +0.2 |
| 1,4,7,10-tetraazadecane 2,2,2-tet | 1 | 9.75 | 9.74 | +0.01 | −45.1 | −45.3 | +0.2 |
| | 2 | 9.07 | 9.13 | −0.06 | −47.2 | −47.4 | +0.2 |
| | 3 | 6.58 | 6.55 | +0.03 | −39.0 | −38.9 | −0.1 |
| | 4 | 3.27 | 3.37 | −0.10 | −29.0 | −28.6 | −0.4 |
| 1,4,7,10,13-pentaazatridecane 2,2,2,2-pent | 1 | 9.76 | 9.76 | 0.00 | −45.1 | −45.1 | 0.0 |
| | 2 | 9.18 | 9.17 | +0.01 | −47.2 | −46.9 | −0.4 |
| | 3 | 8.10 | 8.09 | +0.01 | −44.7 | −44.7 | 0.0 |
| | 4 | 4.65 | 4.66 | −0.01 | −33.0 | −33.1 | +0.1 |
| | 5 | 2.97 | 2.91 | +0.06 | −28.0 | −28.4 | +0.4 |

^aTheir structures are given in Figure 1b. ^bExperimental data taken from a database.⁴⁴

Figure 4d. The dominant singly protonated species is the one where the secondary amine is protonated, which occurs due to its more basic character. But the species where the primary amine is protonated can be also found in substantial quantities. Increasing the temperature shifts the distribution toward the more dominant one. The most prevalent microspecies with two bound protons is the one where the distant primary and secondary amine groups are protonated. The other coexisting species involve the one where the two primary amines are protonated and the one where the two secondary amines are protonated. The species where neighboring primary and secondary amine groups are protonated occurs at negligible concentrations only. The concentration of the major species can again be enhanced by increasing the temperature. The major species where only one site is deprotonated is the one where the secondary amine group is deprotonated. The species with a deprotonated primary amine is also present in substantial amount. Increasing temperature leads to a substantial increase of the concentration of the most dominant species. The microscopic protonation mechanism of 3,4,3-tet suggested by Frassinetti et al.¹³ is closely similar to the one obtained here. In particular, they report exactly the same sequence in the prevalence of the individual microspecies as established here. The agreement between these two independent approaches adds further confidence to the present analysis of a homologous series.

Let us now focus on protonation equilibria and enthalpies of the linear amines 2-di, 2,2-tri, 2,2,2-tet, and 2,2,2,2-pent (Figure 1b). The experimental data at an ionic strength of 0.1 M are summarized in Table 2. The best parametrization of the problem together with the result of the least-squares fit of the data is presented in Figure 5. The model assumes pair interactions between all possible pairs of sites as well as nearest neighbor triplet interactions. The fitted macroconstants and macroenthalpies are given in Table 2. The model describes the data well, most likely within experimental error. This model involves additional pair interactions compared to the ones proposed earlier to describe the protonation constants.¹⁰ This complication is necessary to properly describe the behavior of the stepwise reaction enthalpy sequence $H_1 > H_2 < H_3$, which has already intrigued researchers.⁴⁶

**Figure 5.** Best fit cluster constants and cluster enthalpies for 2-di, 2,2-tri, 2,2,2-tet, 2,2,2,2-pent at an ionic strength of 0.1 M. The cluster enthalpies are reported in kJ/mol.

We distinguish three types of primary amine groups, namely, those neighboring a primary one with a microconstant $pK_a^{(I)} = 9.62$ and a microenthalpy $\hat{H}_a^{(I)} = -49.4$ kJ/mol (in 2-di), neighboring a secondary and subsequently a primary one with $pK_b^{(I)} = 9.43$ and $\hat{H}_b^{(I)} = -47.6$ kJ/mol (in 2,2-tri), and neighboring two secondary ones with $pK_c^{(I)} = 9.38$ and $\hat{H}_c^{(I)} = -46.2$ kJ/mol (in 2,2,2-tet and 2,2,2,2-pent). There are equally three types of secondary amine groups, those neighboring two primary amine groups with a microconstant $pK_a^{(II)} = 8.89$ and a microenthalpy $\hat{H}_a^{(II)} = -41.1$ kJ/mol (in 2,2-tri), those neighboring a primary and a secondary amine group with $pK_b^{(II)} = 8.58$ and $\hat{H}_b^{(II)} = -39.9$ kJ/mol (in 2,2,2-tet and 2,2,2,2-pent), and those neighboring two secondary amine groups with $pK_c^{(II)} = 8.27$ and $\hat{H}_c^{(II)} = -38.8$ kJ/mol (in 2,2,2,2-pent). For

simplicity, we have assumed that one can use the group additivity relationships to estimate $p\hat{K}_b^{(II)} = (p\hat{K}_a^{(II)} + p\hat{K}_c^{(II)})/2$ and $\hat{H}_b^{(II)} = (\hat{H}_a^{(II)} + \hat{H}_c^{(II)})/2$.

We further consider four pair interactions and one triplet interaction. The nearest-neighbor pair interaction parameter is $\varepsilon = 2.20$, and the corresponding pair enthalpy is $g = -4.4$ kJ/mol. The nearest neighbor triplet interaction parameter is $\lambda = 0.25$, and the corresponding triplet enthalpy $l = -2.2$ kJ/mol. The next nearest neighbor pair interactions include those acting across one site (in 2,2-tri, 2,2,2-tet, and 2,2,2,2-pent), across two sites (in 2,2,2-tet and 2,2,2,2-pent), and across three sites (in 2,2,2,2-pent). We approximate all these next nearest neighbor parameters by common values of $\tilde{\varepsilon} = 0.01$ and $\tilde{g} = +1.9$ kJ/mol.

Let us compare the present model results with earlier results concerning the protonation constants of the same series of aliphatic amines obtained by cluster techniques. Some of us have proposed that microconstants of all primary and secondary amine groups are respectively the same, namely, $p\hat{K}_a^{(I)} = p\hat{K}_b^{(I)} = p\hat{K}_c^{(I)} = p\hat{K}^{(I)}$ and $p\hat{K}_a^{(II)} = p\hat{K}_b^{(II)} = p\hat{K}_c^{(II)}$, and that only nearest-neighbor interactions between pairs ε and triplets λ have to be considered.^{10,11} Least-squares fit of the protonation macroconstants of the homologous series up to 2,2,2-tet in the same medium as studied here gave $p\hat{K}^{(I)} = 9.42$, $p\hat{K}^{(II)} = 8.44$, $\varepsilon = 1.97$, and $\lambda = 0.42$.¹⁰ Titration data of 2,2,2,2-pent obtained by Hague et al.²² with ¹³C NMR in D₂O at an ionic strength of 0.2 M were independently analyzed with cluster expansion techniques,¹¹ and the corresponding values were $p\hat{K}^{(I)} = 10.05$, $\varepsilon = 1.97$, and $\lambda = 0.42$. The values of the cluster parameters found here are rather similar, and it is indeed possible to describe the macroconstants with a common microconstant for all primary and secondary amine groups. With this assumption, however, a proper description of the macroenthalpies is impossible. The longer-ranged neighbor pair interactions $\tilde{\varepsilon}$ can also be assumed to vanish to describe the binding constants, but the corresponding pair enthalpy \tilde{g} is essential to rationalize the enthalpies. In particular, the positive enthalpy involving pairs of distant neighbors is essential to capture the stepwise protonation enthalpy sequence $H_1 > H_2 < H_3$. The origin of these interactions might be related to a temperature-dependent conformational transition.

Figure 6 shows the protonation mechanism for 2,2,2,2-pent. The most important intermediate species has three protons bound ($n = 3$). This species dominates over other species at intermediate pH where the two primary and the central secondary amines are protonated. Such alternating microstates are particularly stable in linear polyamines due to the strong nearest neighbor pair repulsion. The stability of the alternating microstates is also reflected in 2,2-tri by the dominance of the doubly protonated species, where the two primary amines are protonated (see supplement). Microstates of 2,2,2,2-pent with one or two bound protons are dominated by the species where primary amines are protonated. Other species coexist in minor quantities. When only one site remains deprotonated, the two species where either the central or the peripheral secondary amine groups is protonated coexist in about the same quantities. When the temperature is increased, the major species is always enhanced. This enhancement is particularly pronounced for the microspecies where the two primary amines are protonated ($n = 2$). Analysis of the NMR data leads exactly to the same sequence in the prevalence of the individual microspecies as established on the basis of the homologous series.¹¹ This agreement with a completely independent

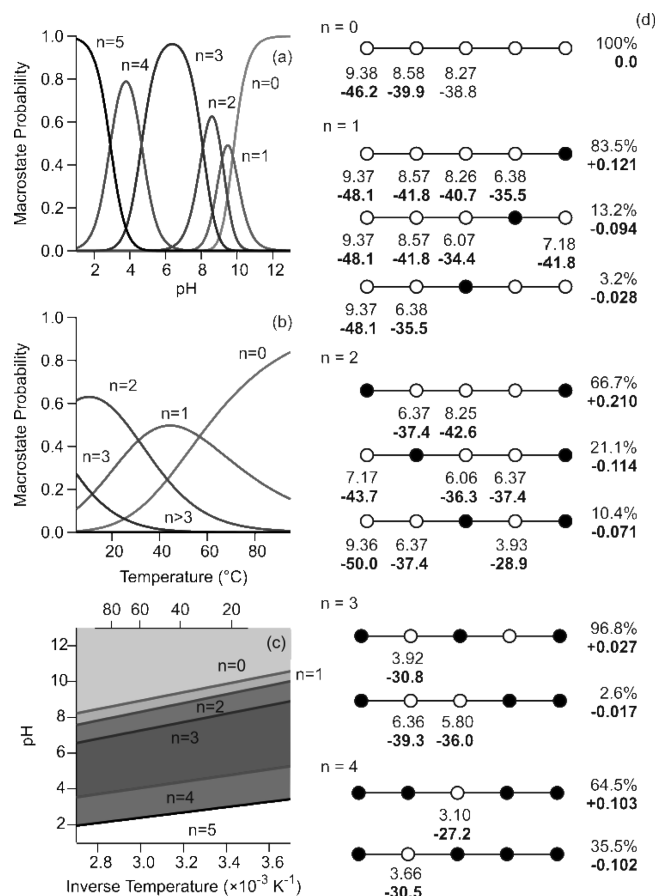


Figure 6. Protonation mechanism of 2,2,2,2-pent at an ionic strength of 0.1 M. Macrostate probabilities for various number n of protons bound (a) as a function of pH at 25 °C and (b) as a function of temperature at pH 9.0. (c) Dominant macrospecies as revealed in the van 't Hoff prevalence diagram. (d) Dominant microstates ordered according to the number n of protons bound. The conditional microstate probability (in %) and its temperature coefficient (bold, in %K⁻¹) are shown on the right. Below each deprotonated site, the respective microconstant and microenthalpy (bold, in kJ/mol) are given.

technique again illustrates the reliability of the present analysis based on the homologous series.

CONCLUSIONS

The present article shows how to obtain microenthalpies of protonation reactions with cluster expansion techniques. The present approach relies on the analysis of macroscopic protonation constants and protonation enthalpies within a homologous series, whereby various linear aliphatic polyamines are considered as examples. We find that in 3,4-tri (spermidine) the primary amine at the butyl rest protonates first, and in a second step the other primary amine protonates. On the other hand, the secondary amine protonates first in 3,4,3-tet (spermine), and is followed by the protonation of the more distant primary amine group. Finally, one secondary amine group is left deprotonated. Within this series, the interactions are weak due to the large distance between the amine groups, and several other microstates coexist with the dominant ones. In the case of 2,2,2,2-pent, the interactions are stronger, and only a few microspecies dominate. The protonation of this molecule proceeds by the protonation of the two primary amines, and by subsequent protonation of the central

secondary amine. The latter microspecies where protonated and deprotonated groups alternate along the chain is particularly stable and dominates the intermediate pH range.

The effects of temperature are twofold. Due to the large negative protonation enthalpy, deprotonated species are favored at higher temperatures. One further observes that the concentrations of dominant microspecies are enhanced with increasing temperature. However, this enhancement is not related to the negative enthalpies, but rather to the differences between microenthalpies of different groups and the respective pair enthalpies.

While the analysis of macroscopic protonation constants and enthalpies within a homologous series represent the most straightforward approach to resolve microconstants and microenthalpies, other approaches to this problem are equally conceivable. In particular, NMR titration techniques have proven very powerful to resolve microscopic equilibria, and we expect that an analogous study of their temperature dependence should provide a possibility to evaluate the microenthalpies. On the other hand, the description of microenthalpies seems to require higher order terms in the cluster expansion, and NMR titration curves at different temperatures may not be sufficient to resolve the microenthalpies fully.

Here, we have focused on the protonation constants pK and enthalpies H , but one could equally consider the enthalpies H and the entropies S , or protonation constants pK and entropies S . These parametrizations are fully equivalent, and we prefer to discuss the first one, as its relation to the description of the microconstants and their temperature dependence is more evident. The corresponding entropies can be always obtained from the Gibbs relation.

■ ASSOCIATED CONTENT

■ Supporting Information

Protonation mechanism for other polyamines and microenthalpies for additional highly symmetric molecules. This material is available free of charge via the Internet at <http://pubs.acs.org>.

■ AUTHOR INFORMATION

Corresponding Author

*Phone: +41 22 379 6405. Fax: + 41 22 379 6069. E-mail: michal.borkovec@unige.ch.

Notes

The authors declare no competing financial interest.

■ ACKNOWLEDGMENTS

D.C. expresses his gratitude to the Swiss National Science Foundation for a stipend, which enabled him to stay for a few months at the University Geneva.

■ REFERENCES

- (1) Ercolani, G. J. *Am. Chem. Soc.* **2003**, *125*, 16097–16103.
- (2) Canard, G.; Koeller, S.; Bernardinelli, G.; Piguet, C. *J. Am. Chem. Soc.* **2008**, *130*, 1025–1040.
- (3) Piguet, C. *Dalton Trans.* **2011**, *40*, 8059–8071.
- (4) Huang, X. Q.; Zheng, F.; Crooks, P. A.; Dwoskin, L. P.; Zhan, C. G. *J. Am. Chem. Soc.* **2005**, *127*, 14401–14414.
- (5) Bazzicalupi, C.; Bianchi, A.; Giorgia, C.; Paz Clares, M.; Garcia-Espana, E. *Coord. Chem. Rev.* **2012**, *256*, 13–27.
- (6) De Sancho, D.; Best, R. B. *J. Am. Chem. Soc.* **2011**, *133*, 6809–6816.

- (7) Feret, J.; Danos, V.; Krivine, J.; Harmer, R.; Fontana, W. *Proc. Natl. Acad. Sci. U.S.A.* **2009**, *106*, 6453–6458.
- (8) Cukrowski, I.; Matta, C. F. *Comput. Theor. Chem.* **2011**, *966*, 213–219.
- (9) Salehzadeh, S.; Gholiee, Y.; Bayat, M. *Int. J. Quantum Chem.* **2011**, *111*, 3608–3615.
- (10) Borkovec, M.; Koper, G. J. M. *J. Phys. Chem.* **1994**, *98*, 6038–6045.
- (11) Borkovec, M.; Koper, G. J. M. *Anal. Chem.* **2000**, *72*, 3272–3279.
- (12) Koper, G. J. M.; van Genderen, M. H. P.; Elissen-Roman, C.; Baars, M. W. P. L.; Meijer, E. W.; Borkovec, M. *J. Am. Chem. Soc.* **1997**, *119*, 6512–6521.
- (13) Frassinetti, C.; Alderighi, L.; Gans, P.; Sabatini, A.; Vacca, A.; Ghelli, S. *Anal. Bioanal. Chem.* **2003**, *376*, 1041–1052.
- (14) Borkovec, M.; Spiess, B. *Phys. Chem. Chem. Phys.* **2004**, *6*, 1144–1151.
- (15) Riley, A. M.; Trusselle, M.; Kuad, P.; Borkovec, M.; Cho, J.; Choi, J. H.; Qian, X.; Shears, S. B.; Spiess, B.; Potter, B. V. L. *ChemBioChem* **2006**, *7*, 1114–1122.
- (16) Cakara, D.; Kleimann, J.; Borkovec, M. *Macromolecules* **2003**, *36*, 4201–4207.
- (17) van Duijvenbode, R. C.; Borkovec, M.; Koper, G. J. M. *Polymer* **1998**, *39*, 2657–2664.
- (18) Onufriev, A.; Case, D. A.; Ullmann, G. M. *Biochemistry* **2001**, *40*, 3413–3419.
- (19) Ullmann, G. M. *J. Phys. Chem. B* **2003**, *107*, 1263–1271.
- (20) Szakacs, Z.; Krasznai, M.; Noszal, B. *Anal. Bioanal. Chem.* **2004**, *378*, 1428–1448.
- (21) Mernissi-Arifi, K.; Schmitt, L.; Schlewer, G.; Spiess, B. *Anal. Chem.* **1995**, *67*, 2567–2574.
- (22) Hague, D. N.; Moreton, A. D. *J. Chem. Soc., Perkin Trans. 2* **1994**, 265–270.
- (23) Kuad, P.; Borkovec, M.; Desage-El Murr, M.; Le Gall, T.; Mioskowski, C.; Spiess, B. *J. Am. Chem. Soc.* **2005**, *127*, 1323–1333.
- (24) Smits, R. G.; Koper, G. J. M.; Mandel, M. *J. Phys. Chem.* **1993**, *97*, 5745–5751.
- (25) van Duijvenbode, R. C.; Rajanayagam, A.; Koper, G. J. M.; Baars, M. W. P. L.; de Waal, B. F. M.; Meijer, E. W.; Borkovec, M. *Macromolecules* **2000**, *33*, 46–52.
- (26) Borkovec, M.; Koper, G. J. M. *Macromolecules* **1997**, *30*, 2151–2158.
- (27) Keszvatera, T.; Jonsson, B.; Thulin, E.; Linse, S. *Proteins* **1999**, *37*, 106–115.
- (28) Niu, Y. H.; Sun, L.; Crooks, R. A. *Macromolecules* **2003**, *36*, 5725–5731.
- (29) Ziebarth, J. D.; Wang, Y. M. *Biomacromolecules* **2010**, *11*, 29–38.
- (30) Garces, J. L.; Koper, G. J. M.; Borkovec, M. *J. Phys. Chem.* **2006**, *110*, 10937–10950.
- (31) Koper, G.; Borkovec, M. *J. Phys. Chem. B* **2001**, *105*, 6666–6674.
- (32) Borkovec, M.; Hamacek, J.; Piguet, C. *Dalton Trans.* **2004**, 4096–4105.
- (33) Zeckert, K.; Hamacek, J.; Rivera, J. P.; Floquet, S.; Pinto, A.; Borkovec, M.; Piguet, C. *J. Am. Chem. Soc.* **2004**, *126*, 11589–11601.
- (34) Piguet, C.; Borkovec, M.; Hamacek, J.; Zeckert, K. *Coord. Chem. Rev.* **2005**, *249*, 705–726.
- (35) Llor, J.; Asensio, S. B. *J. Solution Chem.* **1995**, *24*, 1293–1305.
- (36) Llor, J.; Ros, M. P.; Asensio, S. B. *J. Solution Chem.* **1997**, *26*, 1021–1036.
- (37) Llor, J.; Ros, M. P.; Asensio, S. B. *J. Solution Chem.* **2000**, *29*, 1123–1141.
- (38) Koper, G. J. M.; Minkenberg, C. B.; Upton, I. S.; van Esch, J. H.; Sudholter, E. J. R. *J. Phys. Chem. B* **2009**, *113*, 15597–15601.
- (39) Borkovec, M.; Jonsson, B.; Koper, G. J. M. *Colloid Surface Sci.* **2001**, *16*, 99–339.
- (40) Wyman, J.; Gill, S. J. *Binding and Linkage*; University Science Books: Mill Valley, 1990.

- (41) Hill, T. L. *An Introduction to Statistical Thermodynamics*; Dover: New York, 1987.
- (42) Perrin, D. D.; Dempsey, B.; Serjeant, E. P. *pKa Prediction for Organic Acids and Bases*; Chapman and Hall: New York, 1981.
- (43) Callen, H. B. *Thermodynamics*; John Wiley: New York, 1960.
- (44) Martell, A. E.; Smith, R. M.; Motekaitis, R. J. *Critically Selected Stability Constants of Metal Complexes Database*, version 8.0.; National Institute of Standards and Technology: Gaithersburg, 2004.
- (45) Wallace, H. M.; Fraser, A. V.; Hughes, A. *Biochem. J.* **2003**, 376, 1–14.
- (46) Bencini, A.; Bianchi, A.; Garcia-Espana, E.; Micheloni, M.; Ramirez, J. A. *Coord. Chem. Rev.* **1999**, 188, 97–156.